pH-responsive photoluminescent LbL hydrogels with confined quantum dots†

Eugenia Kharlampieva,[a] Veronika Kozlovskaya,[a] Oleksandra Zavgorodnya,[a] George Daniel Lilly,[b] Nicholas A. Kotov[b] and Vladimir V. Tsukruk*[a]

Received 1st September 2009, Accepted 20th November 2009
First published as an Advance Article on the web 23rd December 2009
DOI: 10.1039/b917845g

We report on responsive photoluminescent hybrid materials with quantum dots immobilized in organized manner fabricated by spin-assisted layer-by-layer assembly (SA LbL). The strongly interacting polyelectrolytes such as poly(allylamine hydrochloride) (PAH) and poly(sodium 4-styrenesulfonate) (PSS) serve for confining CdTe nanoparticles stabilized by thioglycolic acid, while a poly(methacrylic acid) (PMAA) hydrogel matrix presents an elastomeric network with pH-responsive properties. Quantum dot layers encapsulated in PSS-PAH bilayers are confined inside this hybrid hydrogel matrix. The system undergoes reversible changes in photoluminescent intensity in response to pH variations. Photoluminescent intensity of the hybrid matrix is suppressed in excess negative charge at high pH, but excess positive charge at low pH results in significant photoluminescence increase. Such hybrid quantum dot-containing hydrogel-LbL assemblies provide a way for a novel design of materials with precisely controlled structure and pH-triggered optical properties which might be developed into or pH- or chemical sensors.

Introduction

Modern applications require a new design of responsive functional coatings capable of changing their properties in a controlled way under external stimuli.[1] Integration of responsive matrix with functional inorganic nanoparticles offers control over response and structure of the hybrid systems on demand.[2] Surface hydrogels as crosslinked polymer networks capable of uptaking large amounts of water, are typical examples of responsive materials.[3,4] These matrices can provide an ideal environment for hosting a variety of functional molecules and nanoparticles. Even ultrathin hydrogels (<100 nm) possess a high loading capacity, which is along with their fast response to stimuli, offers a wealth of opportunities in drug delivery and sensing.[5–7]

In contrast to other techniques to produce surface hydrogels, for example, a radiation- or chemically-induced attachment of films to functionalized surfaces,[8–11] a layer-by-layer (LbL) assembly allows fabricating hydrogels on any substrate with a thickness control *via* a variation of a number of layers.[12–14] This way, ultrathin surface hydrogels were constructed by polymer assembly with microgel particles,[15,16] by sequential chemical crosslinking of polymers during self-assembly[17,18] or by thermal-, photo-, and chemical cross-linking at a post-assembly step.[19,20] Recently, a microstratified two-component hydrogel-based architecture was obtained by assembly of alginate gels with poly(L-lysine)-hyaluronic acid films.[21] However, despite the unique hydrogel properties such as high loading capacity combined with the fast response, design of stratified hydrogel-based structures capable of incorporating nanoparticles has been rarely explored.

On the other hand, the LbL assembly was intensively used to produce stratified coatings with controllable organization of the incorporated species when polyelectrolytes were assembled with functional moieties. This way, a variety of LbL hybrid nanomaterials have been fabricated by encapsulating nanoparticles, nanosheets, nanowires, or nanorods[22–27] making them promising for biosensing, nonlinear optical devices, memory devices, selective membranes, and for biomedical applications.[28,29]

Among other functional moieties, quantum dots, also known as semiconductor nanocrystals, have been successfully incorporated into a polymeric matrix *via* an alternating assembly with polyelectrolytes giving rise to functional semiconducting films with unique optical properties.[30–34] In contrast to conventional fluorescent dyes, quantum dots possess emission spectra with a narrow and symmetric emission band and have been widely used as photoluminescent component for labeling, imaging, and detection in optoelectronics, biological assays, bio- and chemosensors.[35,36] For example, LbL films emitting light of different colors ("nanorainbows") were prepared by incorporation of quantum dots into polyelectrolyte matrix.[37] Another example includes freely suspended highly fluorescent ultrathin membranes fabricated by embedding a quantum dot monolayer into the LbL film.[38] In the alternative approach, quantum dots were loaded into preassembled LbL polyelectrolyte films at the post-assembly step.[39,40]

Besides the capability to produce stratified structures, LbL films with proper composition might also exhibit a pH-responsive behavior.[41] However, the response of the conventional LbL films is much weaker as that for the hydrogel-based systems. The reason is strong intermolecular interactions in the conventional LbL films, which however, results in stratified structures, but lacks in sensitivity to pH variations. For example, the LbL films of poly(allylamine hydrochloride) (PAH) and poly(sodium

[a]*Georgia Institute of Technology, School of Materials Science and Engineering and School of Polymer, Textile, and Fiber Engineering, Atlanta, GA 30332, USA. E-mail: vladimir@mse.gatech.edu*
[b]*University of Michigan, Department of Chemical Engineering, Biomedical Engineering, and Materials Science and Engineering, Ann Arbor, MI 48109, USA*

† This paper is part of a *Soft Matter* themed issue on Emerging Themes in Soft Matter: Responsive and Active Soft Materials. Guest Editors: Anna C. Balazs and Julia Yeomans

4-styrenesulfonate) (PSS) exhibit a pH-sensitive swelling only when deposited at pH 9.5 when PAH is partially uncharged (pK_b is 9.5–10) and therefore forms loops upon interaction with PSS.[42] As a result, these films can not hold particles inside in the stratified and confined order but release them out in response to pH variations.[43]

Therefore, there is a challenge to produce nanomaterials which would be stimulus-responsive but capable of preserving the particle confinement upon environmental changes at the same time. Previous studies on responsive matrices, based on ether conventional or hydrogel-like LbL films, explored loading functional moieties into pre-formed films which lacks control over internal structure of the produced composites.[5,39,40] To load nanoparticles, as-prepared matrices were immersed into nanoparticle solutions followed by stimulus-triggered release of the particles. For example, PAH-dextran microgel particles assembled with PSS could load and later release CdTe particles in saline solutions. In this case, PAH-dextran microgels served as reservoirs with high loading capacity, capable of reversible swelling–deswelling as a function of ionic strength.[39] Incorporation of nanoparticles[40] or carbon nanotubes[44] into, so called, exponential LbL films which behave largely as gels has recently been demonstrated. An interesting spontaneous stratification behavior was also observed in exponential LbL layers with incorporated alumosilicates.[45] However, in all these cases the degree of control over the stratification patterns needs to improve further.

In our study we report on novel hybrid LbL-based hydrogels with spatial control over the layer organization and utilize these structures for confining quantum dots within LbL multilayer stacks. In contrast to the previous works, which have utilized a pH responsive LbL matrix for particle release, we take advantage of the firm structural control afforded by LbL technique to study a pH responsive behavior of quantum dots which are confined within the PAH-PSS stratum and, therefore, stay inside the matrix upon pH variations (Fig. 1). These hybrid nanostructured materials with the general formula of $(PAH\text{-}PSS)_n$-$(PMAA)_m$ are prepared by sequential assembly of PAH-PSS films in their "passive", pH-insensitive form, with the "active", pH-sensitive poly(methacrylic acid) (PMAA) hydrogels (Fig. 1). The polyelectrolyte films of strongly interacting PAH-PSS bilayers act as a dense nanoscale matrix for incorporation of quantum dots and confine them in a stratified manner. On the other hand, the LbL-derived hydrogel of crosslinked PMAA serves as a global pH-sensitive matrix with a reversibly changing charge balance.

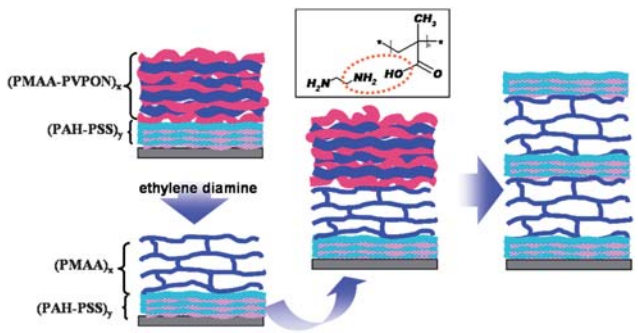

Fig. 1 Fabrication of hybrid hydrogels *via* alternating assembly of electrostatically-bound and hydrogen-bonded (H–B) strata, followed by crosslinking. Inset illustrates crosslinking as a result of interaction of ethylene diamine with carboxylic groups in the H–B strata.

The ultrathin hybrid matrices show controlled and responsive optical properties of quantum dots without compromising their aggregation state. We investigated the role of (1) a number of QD-containing layers, (2) a distance of these layers from the substrate, and (3) a cross-linking density of a PMAA hydrogel stratum on their responsive behavior. To the best of our knowledge this is the first observation of a reversible and robust pH-triggered optical response of quantum dots imbedded into a hybrid matrix made through combining sequential strong-polyelectrolyte and hydrogel interlayers.

Results and discussion

Construction of hybrid LbL-layered hydrogel assembly

To check the feasibility of the approach, we first fabricated a hybrid LbL film composed of chemically cross-linked LbL-derived PMAA hydrogels separated by the electrostatically bound $(PAH\text{-}PSS)_n$ films without quantum dots (Fig. 1).

First, a precursor of a 4.5-bilayer PAH-PSS film is formed on a silicon surface, followed by deposition of a two-component hydrogen-bonded stratum and its subsequent cross-linking to form a one-component PMAA hydrogel. The PAH-PSS film enhances adhesion of the hydrogel to the substrate and at the same time serves as the first pH-insensitive stratum by being deposited at pH 7.5. It was previously shown that PAH-PSS films were insensitive to pH variations if assembled at pH < pK_b of PAH when both polyelectrolytes are in their fully charged state and behave as strong polyelectrolytes.[42,46] Thus, by using the deposition pH = 7.5, we fabricate strata of the electrostatically bound PAH-PSS layers which do not contribute to the responsive behavior of the hybrid system. The PAH-PSS stratum is then capped with the first PMAA layer at pH 7.5. Under these conditions, PMAA carries excess negative charge and interacts with the PAH layer. A hydrogen-bonded stratum of (PMAA-poly-*N*-vinylpyrrolidone) (PMAA-PVPON) is then assembled at pH 3 followed by crosslinking of PMAA. The second electrostatic stratum of a 4.5-layer PAH-PSS film is deposited on top of the PMAA hydrogel starting from PAH at pH 7.5 (see details in the Experimental).

Fig. 2 demonstrates that the hybrid systems grow linearly confirming that polyelectrolyte chains do not diffuse inside the underlying stratum during deposition. Indeed, the SA LbL assembly was shown to produce films with more stratified internal structure than that obtained by the conventional approach of alternating dipping.[47,48] The technique allows a very fast polymer adsorption (~10 s) provided by strong shear forces and a fast solvent removal, factors responsible for the enhanced internal layering of the SA LbL films.[47] Under these conditions, PAH diffusion inside the PMAA hydrogel is kinetically hindered and the polyelectrolyte remains separated, thus, promoting a formation of a stratified layer. The PAH-PSS bilayer thickness of 2.4 nm correlates well with that for the SA LbL film on bare silicon wafers.[47] The whole system was stable with no mass loss in the pH range from 3 to 8.

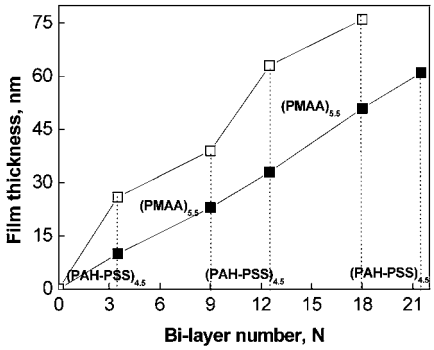

Fig. 2 Layer-by-layer growth of a hybrid matrix by alternating assembly of $(PMMA)_{5.5}$ hydrogels with $(PAH\text{-}PSS)_{4.5}$ films (filled symbols), and the corresponding hybrid matrix with incorporated quantum dots (open symbols).

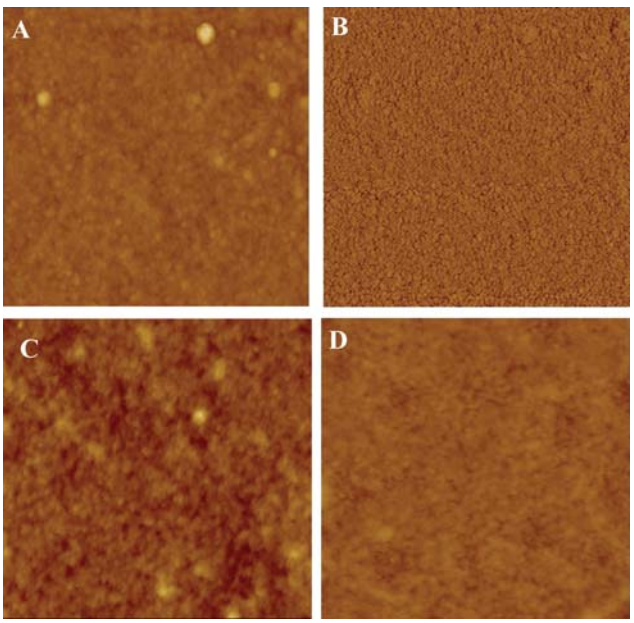

Fig. 3 Topographical (A) and phase AFM image (B) of $(PMAA\text{-}PVPON)_{5.5}$ before crosslinking (A). Topographical images of the film after crosslinking (C) and after coating with $(PAH\text{-}PSS)_{4.5}$ (D). Scan size is $2 \times 2\ \mu m^2$. Height is 50 nm, phase is 50°.

The morphology of the hydrogel surface before and after cross-linking, and after coating with the PAH-PSS film was studied with AFM (Fig. 3). The surface microroughness (within 1 μm^2 surface area) slightly decreased from 1.8 ± 0.2 nm (Fig. 3a) to 1.3 ± 0.2 nm after cross-linking (Fig. 3c). The smoothening of the cross-linked surface occurred due to dissolution of the previously formed hydrogen-bonded complexes between the PMAA and PVPON and overall polymer matrix extension due to increased hydrophilicity of the ionized polyacid chains after PVPON release.[49] Further deposition of the PSS-PAH stratum did not significantly affect the surface morphology (Fig. 3d).

Incorporation of quantum dots

CdTe quantum dots of 2.6 nm in size and stabilized with thioglycolic acid (CdTe-TGA) were incorporated as a single layer into the $(PAH\text{-}PSS)_5$ stratum. Negatively-charged CdTe-TGA quantum dots were readily tethered onto positively charged PAH layers at pH 7.5. In addition, the PMAA hydrogels carrying excess negative charge at pH 7.5 create barriers which prevent diffusion of negatively charged quantum dots from PAH-PSS films. This way, two quantum dot layers introduced into the hybrid LbL-hydrogel matrix were confined within the PAH-PSS stratum and separated by a PMAA hydrogel (Fig. 4). Fig. 4 also illustrates that quantum dots were incorporated as a single layer into the first PAH-PSS stratum, close to the substrate, or into the second stratum, sandwiched in between two hydrogels. The systems are discussed further in detail.

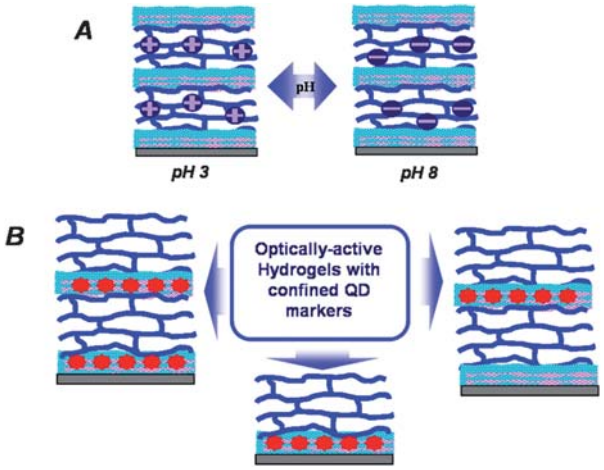

Fig. 4 Variation of pH-Induced charge balance in the hybrid systems (A). Hybrid systems with incorporated quantum dots utilized for the study (B).

Incorporation of quantum dots into $(PAH\text{-}PSS)_5$ multilayer layer results in an increase in layer thickness from 10 to 20 nm before and after the quantum dot incorporation, respectively (Fig. 2). The incremental increase in thickness suggests that nanoparticles, which have dimensions of 2.6 nm in solutions, form aggregates of approximately 10 nm in height upon adsorption on the surface. Similar results on clusterisation of CdS quantum dots into aggregates of 10-nm in height after adsorption onto PAH-tethered surfaces was observed previously, which was attributed to the intercalation of nanoparticles with PAH layers.[50] To avoid the quantum dot aggregation, we also performed their deposition from diluted solutions, which, however, resulted in a significant decrease in photoluminescence intensity. On the other hand, formation of the aggregates upon adsorption is beneficial for positioning nanoparticles within the PAH-PSS stratum, as this prevents their diffusion into a hydrogel stratum whose mesh size is smaller than 10 nm.[51] Moreover, a covalent binding of carboxylic groups of the TGA-capping shell to primary amino groups of PAH, which might occur at the step of hydrogel cross-linking, additionally traps quantum dots inside the PAH-PSS matrix.

The AFM analysis reveals that introducing a quantum dot layer into the first PAH-PSS stratum covered with the hydrogel results in a two-fold increase in surface roughness (up to 3 nm) as compared to the quantum dot-free system (Fig. 5). Further increase in roughness to 4.0 ± 0.3 nm and 3.7 ± 0.3 nm is

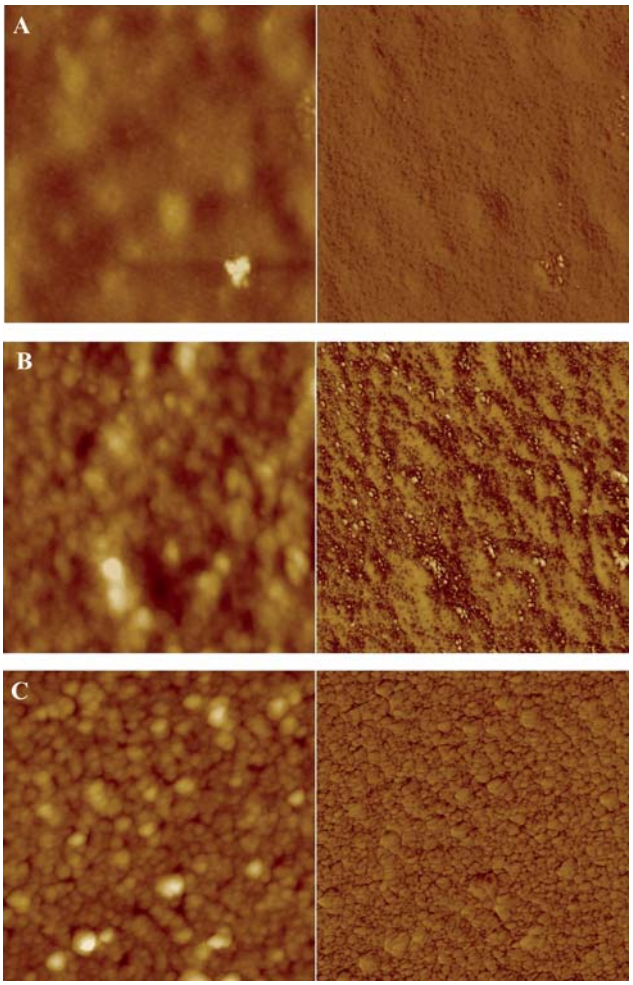

Fig. 5 Topographical (left) and phase AFM images (right) of the systems with one quantum dot layer in the first stratum (A), one quantum dot layer in the second stratum (B), and two quantum dot layers (C). Scan size is 2 × 2 μm². Height is 50 nm, phase is 50°.

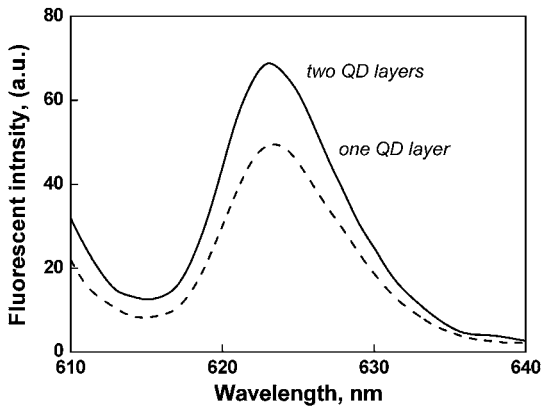

Fig. 6 Photoluminescence spectra of hybrid matrix with one and two layers of quantum dots.

observed for the systems with one "sandwiched" quantum dot layer and two quantum dot layers, respectively (Fig. 5).

A typical photoluminescence spectrum of a quantum dot layer inside the hybrid matrix at pH 7.5 is shown in Fig. 6. The spectrum has a strong emission band centered at 630 nm, typical for CdTe nanoparticles incorporated inside the PAH-PSS multilayers.[39] This result indicates that quantum dots impart a new optical capability on the hybrid matrix which correlates well with previous works on incorporation of quantum dots into LbL films when photoluminescence was preserved in the films.[38,52–54] The band intensity increases with an introduction of a second quantum dot layer and the unchanged peak position indicates no change in quantum dot aggregation state (Fig. 6).

pH-induced variation in hybrid LbL films

The striking feature of the hybrid system containing two quantum dot layers appeared when pH value was reduced to pH 3. Under these conditions the photoluminescent intensity significantly increased, but dropped down again when pH was changed back to pH 8. The unchanged peak position evidences no changes in quantum dot surface structures and no particle aggregation upon the pH variations. The reversible variations of photoluminescence as a function of pH described above are shown in Fig. 7. We did not further decrease pH below 3 because quantum dots were shown to lose their TGA shell as a result of the protonation of thiol groups followed by the ligand detachment.[55,56]

The ability of quantum dots to respond to pH variations (although complicated by quantum dot precipitation) has been reported in the previous studies performed in aqueous solutions.[57–59] The pH-dependent photoluminescent intensity of quantum dots was found to be significantly suppressed in basic solutions but restored at the acidic pH.[35,60] pH-Triggered response of quantum dots was attributed to the pH sensitivity of capping ligands. When the ligands are negatively charged, they exchange electrons and/or energy with the nanoparticles upon excitation and therefore, quench their emission, in contrast to quantum dots without pH-sensitive ligands.[35] The increased photoluminscent intensity at acidic pH can be also attributed to the formation of coordination complexes between cadmium ions and protonated groups on quantum dot surfaces. The increased surface coverage with TGA at acidic pH promotes the formation of thick cadmium thiol complexes which act as a wide band gap material increasing the photoluminescence intensity.[56,58]

The pH-responsive nature of PMAA hydrogels cross-linked *via* carbodiimide chemistry with ethylenediamine (EDA) exploited here has been already described.[61,62] Specifically, the hydrogels exhibited a distinctive polyampholytic behavior as a function of pH, with the minimum swelling at pH = 5, and the maximum film swelling at both the lower and higher pH values. Swelling of the films at high pH was caused by repulsions of negatively charged carboxylic groups which were not involved in crosslinking ($pK_a \sim 6$[63]). Film swelling at acidic pH occurred due to the presence of positively charged ionized primary amino groups ($pK_b \sim 10$)[62] originated from one-end-attachment of EDA crosslinker to PMAA chains, which dominates at low pH as PMAA is protonated.[5,51] In our case we can not attribute the pH-induced change in photoluminescence to swelling–deswelling behavior of the hybrid hydrogels because all experiments are performed in a dry state after the pH treatment. However, PMAA hydrogels were shown to preserve excess charge after drying and found to be negatively or positively charged at pH 8

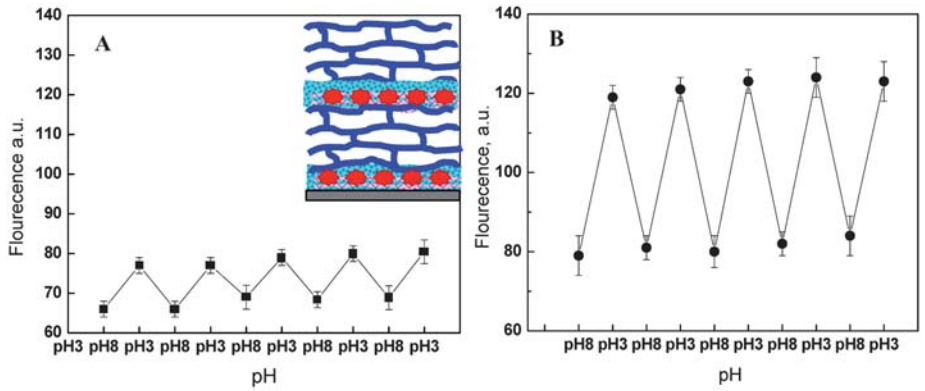

Fig. 7 Variations in photoluminescence intensity as a function of pH for hybrid systems with two quantum dot layers (inset) crosslinked for 10 (A), and 15 h (B).

or 3, respectively (Fig. 2a).[61,62] Therefore, in our case the photoluminescence is suppressed at pH 8 as a result of excess negative charge in the hybrid matrix due to ionized carboxylic groups. However, when the matrix is positively charged at pH 3, the photoluminescence intensity is completely restored.

Interestingly, we found that crosslinking density significantly affects the optical response of the film. With the shorter cross-linking reaction time, the degree of intensity variations was reduced from 34% to 16% (Fig. 7). The results are consistent with the previous finding, when the hydrogel swelling was reduced with an increased cross-linking density.[62] In this case, more positive charges are introduced in the PMAA hydrogel from the EDA cross-linker at a longer cross-linking time, which supports the observed increase in photoluminescence intensity (Fig. 7).

To further investigate the effect of the hydrogel matrix on the photoluminescence intensity, a hybrid system with a single quantum dot layer sandwiched in between two hydrogels was studied as well. A less dramatic variation of the photoluminescence intensity as a function of pH was found for the system with the sandwiched quantum dots layer (Fig. 8). The amplitude of intensity variations was limited to 10% of the peak intensity (Fig. 8). A system with one quantum dot layer close to the substrate and coated with a hydrogel stratum showed even the weaker, 3% variation, in the photoluminescence intensity (Fig. 9). A much weaker variation in the latter case can be attributed to a lower charge density in the surrounding network, indicating that one positively charged hydrogel stratum can not provide excess of positive charges able to induce a noticeable QD response. No significant effect of the cross-linking density on pH-dependent intensity variation was observed due to the fact that we studied dried films in a post-treated fashion (Fig. 8, 9).

Therefore, the pH-triggered change in the photoluminescence intensity is much weaker for the one-QD-layer systems than that for the two-QD-layer hybrid films (Fig. 1). One of the possible explanations would be a variation of Förster resonant energy transfer (FRET) between quantum dot layers. However, FRET is typical to occur between metal particles as strong electron acceptors and quantum dots as donors and results in quenching of photoluminescence or a shift in the emission spectrum.[64] In addition, much shorter distances between a fluorophore and a quencher (<5 nm) are required for the energy transfer mechanism.[64] The close proximity of metal nanoparticles to quantum dots (~5 nm) was also shown to enhance photoluminescence as a result of electromagnetic coupling with surface plasmons.[65] Another example involves solvent-induced fluorescent enhancement when dry poly(2-vinyl pyridine) (P2VP) layers modified with CdSe and deposited on silicon wafers were exposed to organic solvents. This phenomenon was based on fluorescence interference contrast (FLIC) of quantum dots near reflecting surfaces.[36] However, in our case we use a non reflecting glass

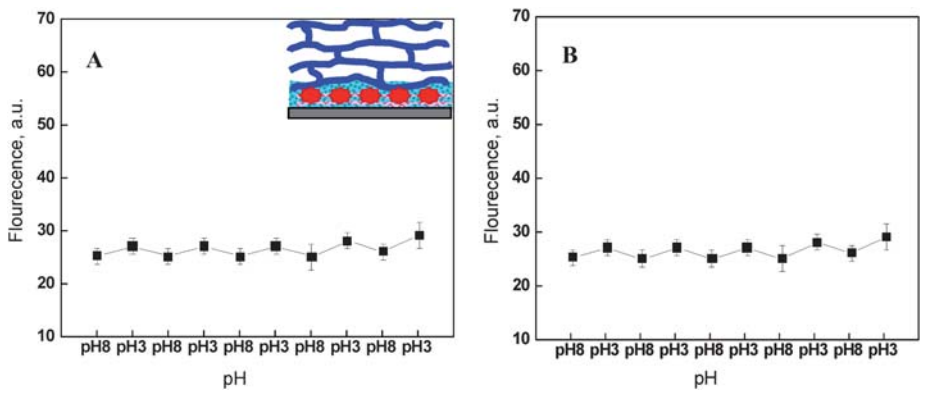

Fig. 8 Variations in photoluminescence intensity as a function of pH for hybrid systems with one quantum dot layer in the first stratum (inset) crosslinked for 10 (A), and 15 h (B).

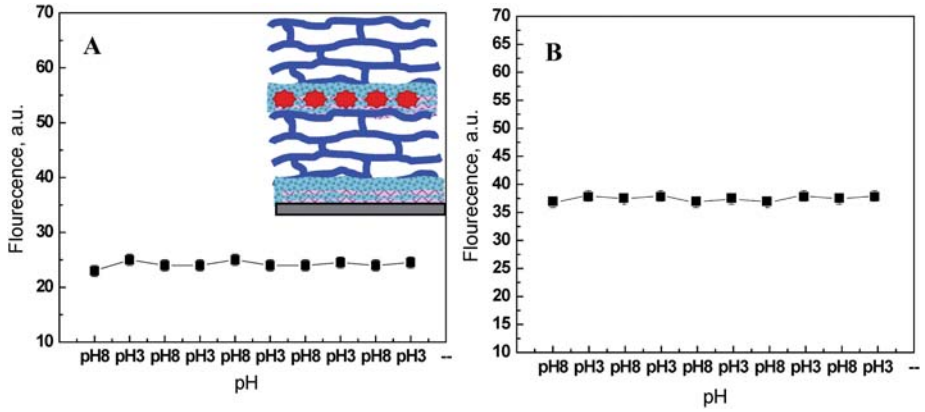

Fig. 9 Variations in photoluminescence intensity as a function of pH for hybrid systems with one quantum dot layer in the second stratum in between two hydrogels (inset) crosslinked for 10 (A), and 15 h (B).

template and the distance between quantum dots remained unchanged with the pH variations as the samples have been dried.

Therefore, we suggest several effects leading to a reversible variation of photoluminescence intensity in the hybrid hydrogels. The first cause is a change in total charge balance provided by the pH responsive hydrogels. Acting through an organic shell, excess negative charge partially quenches the photoluminescence, but positive charge restores the intensity. When the matrix is positively charged, protonation of TGA restores the original pH-responsive behavior of quantum dots, suppressed at high pH, which is similar to the mechanism proposed in TGA-quantum dots in solutions.[66] Indeed, ligands ionized at high pH donate electrons to the excited quantum dots which partially quench their photoluminescence.[35] Increase in the intensity can also be attributed the to additional passivation of quantum dot surfaces by the protonated TGA shell which effectively diminishes the contribution of the non-radiative channels. A similar effect of the increased photoluminescence intensity at acidic pH was observed for CdTe immobilized in p(NIPAM-co-acrylate) networks and was attributed to formation of a dense shell, rich in -COOH groups, which wraps quantum dots and therefore, modifies their photoluminescent properties.[67] At the same time, the change in the intensity is much more pronounced in the case of two-QD-layer films, than in one-QD-layer systems. This effect can originate from interaction between particle dipoles created by the proximity of quantum dot layers.[68]

Conclusions

A hybrid pH-responsive matrix was fabricated by the SA LbL approach through combining strongly bound polyelectrolyte stratums with weakly-bound hydrogel stacks. In contrast to previous studies, which utilized LbL films for reversible pH-triggered loading and release of quantum dots, we demonstrate the application of our pH-responsive hybrid systems for incorporation of quantum dots in a confined environment in a controlled way. We found that these ultrathin hybrid nanostructures exhibit reversible changes in the photoluminescent intensity in the form of variations of the intensity under pH changes from 3 to 8. This response can be tuned by variable hydrogel structure and is found to be suppressed in excess negative charge but significantly increased in the presence of excess positive charge in the hydrogel matrix. The effect is much more pronounced when two quantum dot layers are immobilized in the matrix. The approach presented here allows controlling the architecture of the hybrid systems by the simple manipulation of thickness of both PSS-PAH and PMAA layers. The main advantage of the design suggested here is the robust and reversible optical response which offers a possibility for development of the quantum dot-containing organized hydrogels for prospective pH- sensor or pH-monitoring.

Experimental

Materials

PMAA (Mw = 150 kDa), PVPON (Mw = 55 kDa), PAH (Mw = 60 kDa), PSS (Mw = 70 kDa), 1-ethyl-3-(3-dimethylaminopropyl) carbodiimide hydrochloride (EDC), N-hydroxy-sulfosuccinimide sodium salt (NSS), ethylenediamine (EDA), were purchased from Sigma-Aldrich. To control pH, 0.1M HCl, 0.1M NaOH, and the inorganic salts Na_2HPO_4 and NaH_2PO_4 (Sigma-Aldrich) were utilized as received. Ultrapure (Nanopure system) filtered water with a resistivity 18.2 MΩ cm was used in all experiments. Glass microscope fused slides (Alfa Aesar) were cut by typical size of 10 × 20 mm and cleaned as described elsewhere.[51]

Fabrication of hybrid LbL matrices

All polymer layers were deposited by SA LbL from 0.5 mg mL^{-1} solutions.[69] To perform deposition, 3 mL shots of a polyelectrolyte solution were sequentially dropped on a glass substrate and rotated for 20 s at 3000 rpm on a spin-coater (Laurell Technologies) then rinsed twice with Nanopure buffer followed by the deposition of the next layer. First, 4.5-bilayer electrostatically-bound PAH-PSS film was deposited on the glass substrate at pH 7.5 starting with PAH, followed by deposition of hydrogen-bonded stratum of $(PMAA\text{-}PVPON)_{5.5}$ at pH 3. After the hydrogen-bonded multilayer was formed, it was chemically cross-linked with EDA as has been developed in previous studies and described in detail elsewhere.[49,51] Briefly, the system was

immersed into solution of EDC and NSS at pH 5 for 30 min to activate the carboxylic groups of PMAA and then transferred into 5 mg mL^{-1} EDA solution at pH 5 for 20 h to introduce amide linkages between EDA molecules and the activated carboxylic groups. After the crosslinking reaction was completed, the substrates with tethered hydrogel films were immersed in a 0.01 M buffer solution at pH 8 for one hour to ensure release of PVPON. The PMMA was then coated with the second stratum of a 4.5-bilayer PAH-PSS film at pH 7.5 and with the second stratum of $(PMAA\text{-}PVPON)_5$ at pH 3, followed by crosslinking.

Synthesis of CdTe nanoparticles

TGA-stabilized CdTe nanoparticles were prepared according to the literature procedure.[70,71] H_2Te gas, generated by the reaction of 0.5 M H_2SO_4 and Al_2Te_3 under an N_2 atmosphere, is bubbled through a 1.88×10^{-2} M $Cd(ClO_4)_2 \cdot H_2O$ and 4.56×10^{-2} M TGA solution that has been adjusted to pH 11.4. The resulting CdTe QD solution is refluxed until the quantum dots have an average diameter of 2.6 ± 0.75 nm.

Incorporation quantum dots into LbL hybrid matrix

Quantum dots were deposited at PAH-tethered films from 10^{-5} M at pH 7.5 followed by intensive rinsing with buffer. The first quantum dot (QD) layer was deposited on $(PAH\text{-}PSS)_{3.5}$ stratum followed by coating with $(PAH\text{-}PSS)_{2.5}$ multilayer and further construction of PMAA matrix on top. The second QD layer was introduced in between two films of $(PAH\text{-}PSS)_{2.5}$. This way three systems were used for the study: one-QD-layer (QDs are in the first stratum close to the substrate), one-QD-layer (QDs are in the second stratum sandwiched in between two hydrogels), and two-QD-layer with the corresponding formulas $(PAH\text{-}PSS)_{3.5}QDs(PAH\text{-}PSS)_{2.5}(PMAA)_5$, $(PAH\text{-}PSS)_{4.5}(PMAA)_{5.5}(PAH\text{-}PSS)_{2.5}QDs(PAH\text{-}PSS)_{2.5}(PMAA)_5$, and $(PAH\text{-}PSS)_{3.5}QDs(PAH\text{-}PSS)_{2.5}(PMAA)_{5.5}(PAH\text{-}PSS)_{2.5}QDs(PAH\text{-}PSS)_{2.5}(PMAA)_5$.

Characterization

Photoluminescence spectra were acquired with spectrofluorophotometer RF-5301PC (Shimadzu). Quartz cuvettes (1 cm path length) were utilized to obtain measurements from quantum dot solutions. The measurements of the hybrid LbL coatings were done on glass substrates. Photoluminescence spectra for all samples were obtained in dry state at identical conditions. For the measurements the samples were immersed into solutions with an adjusted pH for 30 min followed by drying with nitrogen. The degree of variation was calculated taking fluorescence at maximum as reference (100%).

AFM images were collected on dry samples using a Dimension-3000 (Digital Instruments) microscope in the tapping mode according to the established procedure.[72]

Acknowledgements

This work is supported by the Air Office of Scientific Research FA9550-08-1-0446 and FA9550-09-1-0162 projects, and NSF-CBET-NIRT 0650705 grant.

References

1 I. Luzinov, S. Minko and V. V. Tsukruk, *Prog. Polym. Sci.*, 2004, **29**, 635.
2 I. Luzinov, S. Minko and V. V. Tsukruk, *Soft Matter*, 2008, **4**, 714.
3 Y. Osada, J. P. Gong and Y. Tanaka, *J. Macromol. Sci.: Polymer Reviews*, 2004, **44**, 87.
4 N. Peppas and W. Leobandung, *J. Biomater. Sci., Polym. Ed.*, 2004, **15**, 125.
5 E. Kharlampieva, I. Erel-Unal and S. A. Sukhishvili, *Langmuir*, 2007, **23**, 175.
6 I. Tokarev and S. Minko, *Adv. Mater.*, 2009, **21**, 241.
7 D. Julthongpiput, Y.-H. Lin, J. Teng, E. R. Zubarev and V. V. Tsukruk, *J. Am. Chem. Soc.*, 2003, **125**, 15912.
8 A. Revzin, R. J. Russell, V. K. Yadavalli, W. G. Koh, C. Deister, D. D. Hile, M. B. Mellott and M. V. Pishko, *Langmuir*, 2001, **17**, 5440.
9 D. Kuckling, M. E. Harmon and C. W. Frank, *Macromolecules*, 2002, **35**, 6377.
10 P. Krsko, S. A. Sukhishvili, M. Mansfield, R. Clancy and M. Libera, *Langmuir*, 2003, **19**, 5618.
11 R. Toomey, D. Freidank and J. Rühe, *Macromolecules*, 2004, **37**, 882.
12 V. V. Tsukruk, *Prog. Polym. Sci.*, 1997, **22**, 247.
13 C. Jiang, S. Markutsya, Y. Pikus and V. V. Tsukruk, *Nat. Mater.*, 2004, **3**, 721.
14 Multilayer Thin Films: *Sequential Assembly of Nanocomposite Materials*, ed. G. Decher, J. B. Schlenoff, Wiley-VCH, Weinheim, 2002.
15 M. J. Serpe and L. A. Lyon, *Chem. Mater.*, 2004, **16**, 4373.
16 M. J. Serpe, K. A. Yarmey, Ch. M. Nolan and L. A. Lyon, *Biomacromolecules*, 2005, **6**, 408.
17 T. Serizawa, Y. Nakashima and M. Akashi, *Macromolecules*, 2003, **36**, 2072.
18 T. Serizawa, D. Matsukuma, K. Nanameki, M. Uemura, F. Kurusu and M. Akashi, *Macromolecules*, 2004, **37**, 6531.
19 S. Y. Yang and M. Rubner, *J. Am. Chem. Soc.*, 2002, **124**, 2100.
20 V. Kozlovskaya, S. Ok., A. Sousa, M. Libera and S. A. Sukhishvili, *Macromolecules*, 2003, **36**, 8590.
21 H. Mjahed, C. Porcel, B. Senger, A. Chassepot, P. Netter, P. Gillet, G. Decher, J.-C. Voegel, P. Schaaf, N. Benkirane-Jessel and F. Boulmedais, *Soft Matter*, 2008, **4**, 1422.
22 E. Kharlampieva and S. A. Sukhishvili, *J. Macromol. Sci.: Polymer Reviews*, 2006, **46**, 377.
23 Z. Tang, Y. Wang, P. Podsiadlo and N. A. Kotov, *Adv. Mater.*, 2006, **18**, 3203.
24 A. P. R. Johnston, C. Cortez, A. S. Angelatos and F. Caruso, *Curr. Opin. Colloid Interface Sci.*, 2006, **11**, 203.
25 C. Jiang, S. Markutsya, H. Shulha and V. V. Tsukruk, *Adv. Mater.*, 2005, **17**, 1669.
26 R. Gunawidjaja, C. Jiang, H. Ko and V. V. Tsukruk, *Adv. Mater.*, 2006, **18**, 2895.
27 R. Gunawidjaja, H. Ko, C. Jiang and V. V. Tsukruk, *Chem. Mater.*, 2007, **19**, 2007.
28 J. Lutkenhaus and P. Hammond, *Soft Matter*, 2007, **3**, 804.
29 C. Jiang and V. V. Tsukruk, *Adv. Mater.*, 2006, **18**, 829.
30 V. Zucolotto, K. M. Gatta's-Asfura, T. Tumolo, A. C. Perinotto, P. A. Antunes, C. J. L. Constantino, M. S. Baptista, R. M. Leblanc and O. N. Oliveira Jr., *Appl. Surf. Sci.*, 2005, **246**, 397.
31 M. T. Crisp and N. A. Kotov, *Nano Lett.*, 2003, **3**, 173.
32 P. Yang, C. L. Li and N. Murase, *Langmuir*, 2005, **21**, 8913.
33 Z. Liang, K. L. Dzienis and Q. Wang, *Adv. Funct. Mater.*, 2006, **16**, 542.
34 S. Lee, B. Lee, B. J. Kim, J. Park, M. Yoo, W. K. Bae, K. Char, C. J. Hawker, J. Bang and J. Cho, *J. Am. Chem. Soc.*, 2009, **131**, 2579.
35 I. Yildiz, M. Tomasulo and F. M. Raymo, *J. Mater. Chem.*, 2008, **18**, 5577.
36 L. Ionov, S. Sarpa, A. Synytska, A. L. Rogach, M. Stamm and S. Diez, *Adv. Mater.*, 2006, **18**, 1453.
37 A. A. Mamedov, A. Belov, M. Giersig, N. N. Mamedova and N. A. Kotov, *J. Am. Chem. Soc.*, 2001, **123**, 7738.
38 D. Zimnitsky, C. Jiang, Z. Xu, Z. Lin, L. Zhang and V. V. Tsukruk, *Langmuir*, 2007, **23**, 10176.
39 L. Wang, X. Wang, M. Xu, D. Chen and J. Sun, *Langmuir*, 2008, **24**, 1902.
40 S. Srivastava, V. Ball, P. Podsiadlo, J. Lee, P. Ho and N. A. Kotov, *J. Am. Chem. Soc.*, 2008, **130**, 3748.

41 S. A. Sukhishvili, *Curr. Opin. Colloid Interface Sci.*, 2005, **10**, 37.
42 J. Hiller and M. F. Rubner, *Macromolecules*, 2003, **36**, 4078.
43 A. J. Chung and M. F. Rubner, *Langmuir*, 2002, **18**, 1176.
44 S. Srivastava, P. Podsiadlo, K. Critchley, J. Zhu, M. Qin, B. S. Shim and N. A. Kotov, *Chem. Mater.*, 2009, **21**, 4397.
45 P. Podsiadlo, M. Michel, K. Critchley, S. Srivastava, M. Qin, J. W. Lee, E. Verploegen, A. J. Hart, Y. Qi and N. A. Kotov, *Angew. Chem.*, 2009, **48**, 7073.
46 K. Itano, J. Choi and M. F. Rubner, *Macromolecules*, 2005, **38**, 3450.
47 E. Kharlampieva, V. Kozlovskaya, J. Chan, J. F. Ankner and V. V. Tsukruk, *Langmuir*, 2009, **25**, 14017.
48 J. Cho, K. Char, J.-D. Hong and K.-B. Lee, *Adv. Mater.*, 2001, **13**, 1076.
49 V. Kozlovskaya, E. Kharlampieva, B. P. Khanal, P. Manna, E. R. Zubarev and V. V. Tsukruk, *Chem. Mater.*, 2008, **20**, 7474.
50 A. Suryajaya, A. Nabok, F. Davis, A. Hassan, S. P. J. Higson and J. Evans-Freeman, *Appl. Surf. Sci.*, 2008, **254**, 4891.
51 V. Kozlovskaya, E. Kharlampieva, M. L. Mansfield and S. A. Sukhishvili, *Chem. Mater.*, 2006, **18**, 328.
52 N. A. Kotov, I. Dekany and J. H. Fendler, *J. Phys. Chem.*, 1995, **99**, 13065.
53 D. Zimnitsky, C. Jiang, Z. Xu, Z. Lin and V. V. Tsukruk, *Langmuir*, 2007, **23**, 4509.
54 C. A. Constantine, K. M. Gatta's-Asfura, S. V. Mello, G. Crespo, V. Rastogi, T.-C. Cheng, J. J. DeFrank and R. M. Leblanc, *J. Phys. Chem. B*, 2003, **107**, 13762.
55 Y. Zhang, L. Mi, P.-N. Wang, J. Ma and J.-Y. Chen, *J. Lumin.*, 2008, **128**, 1948.
56 A. Mandal and N. Tamai, *J. Phys. Chem. C*, 2008, **112**, 8244.
57 Y.-Q. Wang, C. Ye, Z.-H. Zhu and Y.-Z. Hu, *Anal. Chim. Acta*, 2008, **610**, 50.
58 M. Gao, S. Kirstein, H. Möhwald, A. L. Rogach, A. Kornowski, A. Eychmüller and H. Weller, *J. Phys. Chem. B*, 1998, **102**, 8360.
59 A. S. Susha, A. M. Javier, W. J. Parak and A. L. Rogach, *Colloids Surf., A*, 2006, **281**, 40.
60 H. Zhang, Z. Zhou, B. Yang and M. Gao, *J. Phys. Chem. B*, 2003, **107**, 8.
61 V. Kozlovskaya, A. Shamaev and S. A. Sukhishvili, *Soft Matter*, 2008, **4**, 1499.
62 V. Kozlovskaya and S. A. Sukhishvili, *Macromolecules*, 2006, **39**, 6191.
63 D. Pristinski, V. Kozlovskaya and S. A. Sukhishvili, *J. Chem. Phys.*, 2005, **122**, 014907.
64 S. Singamaneni, C. Jiang, E. Merrick, D. Kommireddy and V. V. Tsukuk, *J. Macromol. Sci., Part B: Phys.*, 2007, **46**, 7.
65 Y.-H. Chan, J. Chen, S. E. Wark, S. L. Skiles, D. H. Son and J. D. Batteas, *ACS Nano*, 2009, **3**, 1735.
66 D. M. Guldi, I. Zilbermann, G. Anderson, N. A. Kotov, N. Tagmatarchis and M. Prato, *J. Am. Chem. Soc.*, 2004, **126**, 14340.
67 M. Agrawal, J. Rubio-Retama, N. E. Zafeiropoulos, N. Gaponik, S. Gupta, V. Cimrova, V. Lesnyak, E. López-Cabarcos, S. Tzavalas, R. Rojas-Reyna, A. Eychmüller and M. Stamm, *Langmuir*, 2008, **24**, 9820.
68 J. Kimura, T. Uematsu, S. Maenosono and Y. Yamaguchi, *J. Phys. Chem. B*, 2004, **108**, 13258.
69 S. Markutsya, C. Jiang, Y. Pikus and V. V. Tsukruk, *Adv. Funct. Mater.*, 2005, **15**, 771.
70 N. Gaponik, D. V. Talapin, A. L. Rogach, K. Hoppe, E. V. Shevchenko, A. Kornowski, A. Eychmuller and H. Weller, *J. Phys. Chem. B*, 2002, **106**, 7177.
71 D. V. Talapin, A. L. Rogach, E. V. Shevchenko, A. Kornowski, M. Haase and H. Weller, *J. Am. Chem. Soc.*, 2002, **124**, 5782.
72 V. V. Tsukruk and D. H. Reneker, *Polymer*, 1995, **36**, 1791.